JOURNAL OF APPLIED ELECTROCHEMISTRY 25 (1995) 764–769

# Improved current efficiency equation for the electrodeposition of copper

H. VOGT

*Fachbereich Verfahrens-und Umwelttechnik, Technische Fachhochschule Berlin, D-13353 Berlin, Germany*

Received 3 October 1994; revised 30 January 1995

The current efficiency of copper deposition is controlled by the extent of the competing hydrogen formation reaction which acts on mass transfer of copper ions together with further mass transfer mechanisms. An available current efficiency equation taking account only of the bubble-induced microconvection fails in the case of forced electrolyte flow. The equation is now extended to all other mechanisms. Results are compared with experimental data.

**List of symbols**

$c$ concentration ($mol\,m^{-3}$)
$C_1$ constant, Equation 15 ($m^2\,s^{-1}\,A^{-0.5}$)
$d$ bubble break-off diameter (m)
$D$ diffusion coefficient ($m^2\,s^{-1}$)
$d_h$ equivalent diameter (m)
$F$ Faraday constant ($F = 96\,487\,C\,mol^{-1}$)
$f_G$ gas evolution efficiency (–)
$g$ acceleration due to gravity ($m\,s^{-2}$)
$j$ total current density ($A\,m^{-2}$)
$j_1$ partial current density of copper deposition ($A\,m^{-2}$)
$j_2$ partial current density of hydrogen formation ($A\,m^{-2}$)
$k$ overall mass transfer coefficient of copper ion, Equation 16 ($m\,s^{-1}$)
$k_b$ microconvection mass transfer coefficient ($m\,s^{-1}$)
$k_n$ natural convection mass transfer coefficient ($m\,s^{-1}$)
$k_v$ macroconvection mass transfer coefficient ($m\,s^{-1}$)
$K_1$ dimensionless group, Equation 19
$K_2$ dimensionless group, Equation 20
$K_3$ dimensionless group, Equation 26
$K_M$ migration factor (–)
$L$ characteristic length in natural convection (m)
$L_h$ channel length (m)
$n$ charge number (–)
$p$ pressure ($kg\,m^{-1}\,s^{-2}$)
$R$ universal gas constant ($R = 8.3143\ kg\,m^2\,s^{-2}\,mol^{-1}\,K^{-1}$)
$T$ temperature (K, °C)
$v$ flow velocity ($m\,s^{-1}$)
$X$ dimensionless parameter, Equation 22

*Greek letters*
$\alpha$ expansion coefficient ($m^3\,mol^{-1}$)
$\epsilon$ current efficiency (–)
$\theta$ fractional shielding of the electrode surface (–)
$\nu$ stoichiometric number
$\nu_L$ kinematic viscosity of liquid ($m^2\,s^{-1}$)

*Transport numbers*
$Re$ Reynolds number, Equation 11
$Re_G$ Reynolds number of gas evolution, Equation 13
$Sc$ Schmidt number, Equations 5 and 6
$Sh$ Sherwood number, Equations 4, 10 and 12

*Subscripts*
B dissolved hydrogen
C copper ion
c critical
G gas
$\infty$ liquid bulk

## 1. Introduction

Industrial high-rate deposition of copper is commonly operated with current efficiencies considerably smaller than unity. The competing loss reaction is the formation of hydrogen. This reaction is not simply detrimental in that it lowers the current efficiency. It is tolerated to gain large productivity rates in that it acts beneficially with respect to the increase in the limiting current density of copper deposition. These facts can be elucidated on the basis of the interfering mass transfer mechanisms of copper ions and dissolved hydrogen.

It is the object of the present paper to show how, and to what extent, the mass transfer of copper ions to the cathode is affected by various mechanisms and how the competing hydrogen evolution affects the mass transfer. The present paper will discuss this effect qualitatively and quantitatively. Results are compared with those of a previous restricted investigation [1]. The present theoretical results are finally compared with experimental literature data.

## 2. The ranges of mass transfer

The potential of a cathode, where copper is deposited from a sulfuric electrolyte solution, is shown as line 1



0021-891X/93 

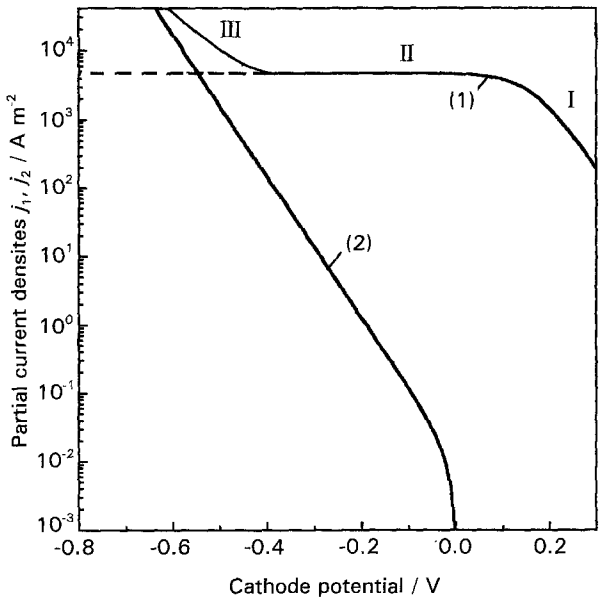


Fig. 1. Partial current densities of the copper deposition (line 1) and of the competing hydrogen formation (line 2).

in Fig. 1. At low values of the cathodic current density for copper deposition, $j_1$, the charge transfer step is the controlling mechanism, (region I). As the current density is increased the interfacial concentration of copper ions in the solution approaches zero. The process becomes mass transfer controlled. Copper deposition occurs at limiting current conditions [2, 3]. The current density approaches a constant limiting value independent of potential, (region II). The mass transfer is affected either by free convection alone (owing to concentration gradients in the boundary layer) or by the combined action of free and forced convection. The latter case is common in industrial application. Inasmuch as the flow velocity of the liquid is not varied and the mass transfer coefficient is constant, the current density remains unchanged, although the electrode potential is shifted.

The situation changes, as the potential attains values where hydrogen formation starts as a competing cathode reaction. Hydrogen formation causes an increase in the rate of mass transfer. Electrodeposition of copper continues to occur at limiting current conditions, but the limiting current density is no longer constant but increases since the mass transfer coefficient is increased. In this range, the increase in mass transfer is not necessarily linked with the formation of gas bubbles. The concentration gradients resulting from the formation of dissolved hydrogen cause a superimposed free convection in addition to the free convection resulting from concentration gradients of copper ions due to depletion at the electrode surface. Although hydrogen bubbles are formed at very low (partial) current densities [4], their microconvective effect is negligible compared to that of liquid-phase free convection at low values of the partial current density of the hydrogen formation. This finding has been made on the basis of theoretical investigations [5] and is confirmed by comparison with experimental results [6].

As the potential is further shifted to more negative values, the microconvection associated with the growth and departure of gas bubbles from the electrode steadily increases and soon exceeds the effect of liquid-phase free convection. Both hydrogen-induced transfer mechanisms act jointly on mass transfer of copper ions to the electrode together with forced convection and copper-induced free convection, as outlined above. The mass transfer coefficient for copper and, hence, the limiting current density for copper deposition, increase drastically, (region III). The effect is the stronger, the larger the partial current density of hydrogen formation, $j_2$ (i.e., the larger the total current density).

The following treatment supposes that the only loss of current efficiency is caused by the competing hydrogen formation reaction. With the total current density

$$j = j_1 + j_2 \tag{1}$$

being composed of the partial current densities $j_1$ of copper deposition (Reaction 1) and $j_2$ of the hydrogen formation (Reaction 2), the current efficiency for copper deposition is defined as

$$\epsilon \equiv \frac{j_1}{j} = \frac{j_1}{j_1 + j_2} = 1 - \frac{j_2}{j} \tag{2}$$

It is seen from Fig. 1, that the current efficiency decreases as the total current density increases, but the decrease is smaller than would be the case if the limiting current density were constant. The competing hydrogen evolution permits operation at current densities which are larger than the maximum current density in the absence of hydrogen formation.

For a quantitative investigation, it is necessary to consider the various competing mass transfer mechanisms. The region III of Fig. 1, where the hydrogen evolution predominates in mass transfer, is the area of concern in this work.

### 3. Active mass transfer mechanisms

At limiting current density, represented by the regions II and III, where the copper concentration, $c_{Cw}$, at the electrode-liquid interface is negligibly small compared to the bulk concentration, $c_{C\infty}$, the partial current density for copper deposition (Reaction 1) is given by

$$j_1 = (n/\nu)_C F k c_{C\infty} K_M \tag{3}$$

The multiplier $K_M$ takes account of the effect of migration on mass transfer. The mass transfer coefficient of the copper ions, $k$, is affected by several mechanisms acting simultaneously to different extents. These are (i) free convection owing to concentration gradients in the boundary layer, (ii) macroconvection owing to fluid flow through the interelectrode gap without or with enhancement by pumping, and (iii) microconvection owing to the microevents in the vicinity of bubbles adhering to the electrode surface. Each of these mass transfer

mechanisms is described by a particular mass transfer coefficient to be calculated separately.

### 3.1. *Liquid-phase free convection*

It has recently been pointed out that the generally disregarded mechanism of free convection plays an important role at gas evolving electrodes. Free convection is induced by concentration gradients in the liquid phase resulting from reactant depletion at the electrode (here copper ions). The effect is enhanced by the depletion of hydrogen ions and by enrichment of dissolved hydrogen at the electrode–electrolyte interface. The resulting free flow in the boundary layer may affect the controlling mass transfer mechanism up to current density values of $1\,\mathrm{kA\,m^{-2}}$ [6]. In this case, the mass transfer equation is [5]

$$Sh_n \equiv \frac{k_n L}{D_C} = 0.72\left[\frac{j_2 \alpha g L^4}{(n/\nu)_B F \nu_L^3}\right]^{0.2} Sc_B^{0.15} Sc_C^{0.25} \times (1-\theta)^{0.8}(1-2/3f_G)^{0.2} \quad (4)$$

where $(n/\nu)_B$ refers to the competing reduction of hydrogen ions (Reaction 2). The subscripts B denote the dissolved hydrogen, C the copper ions. The characteristic length, $L$, is affected by the distance between two neighbouring gas bubbles and, hence, depends on the bubble population density [5], but is of little effect, as seen from the exponent 0.2. Values of the isothermal expansion coefficient, $\alpha$, are often not easily to be found in the literature, but can be predicted from a recently presented method [7]. The Schmidt numbers are defined by

$$Sc_B = \frac{\nu_L}{D_B} \quad (5)$$

$$Sc_C = \frac{\nu_L}{D_C} \quad (6)$$

The fraction, $\theta$, of the total electrode surface area shielded by adhering bubbles can be estimated tentatively from

$$\theta = \left(\frac{j_2}{j_{2c}}\right)^{0.28} \quad (7)$$

where the critical current density $j_{2c} \approx 200\,\mathrm{kA\,m^{-2}}$. The gas evolution efficiency, $f_G$, takes account of the fact that only a fraction of the total hydrogen formed is transferred into the gaseous phase of bubbles adhering to the electrode [8] and may be estimated from [9]

$$f_G = 1 - (1-\theta)^{2.5} \quad (8)$$

Equation 4 applies to a laminar boundary layer valid in the range [5]

$$\frac{j_2 \alpha g L^4}{(n_2/\nu_B) F \nu_L D_B^{0.75} D_C^{1.25}} < 1.2 \times 10^9 \quad (9)$$

### 3.2. *Forced macroconvection*

The mass transfer of copper ions induced by liquid flow or liquid–gas flow past the electrode surface can be described by one of the numerous available mass transfer equations, for example, for single-phase turbulent flow in a channel by [10]

$$Sh_v \equiv \frac{k_v d_h}{D_C} = 0.037(Re^{0.75} - 180) Sc_C^{0.42}[1 + (d_h/L_h)^{2/3}](1-\theta) \quad (10)$$

where the Reynolds number is

$$Re \equiv \frac{v d_h}{\nu_L} \quad (11)$$

The characteristic geometric length is now the equivalent diameter $d_h$, $L_h$ denotes the length of the flow channel, where $v$ is the mean flow velocity.

### 3.3. *Bubble-induced microconvection*

Bubble growth accompanied by a radial liquid flow past the surface and bubble breakoff from the electrode accompanied by a violent wake exerts a further mass transfer mechanism. This mechanism can be described by [8, 11]

$$Sh_b = \frac{k_b d}{D_C} = 1.89[Re_G f_G \theta^{0.5}(1-\theta^{0.5})]^{0.5} Sc_C^{0.487} \quad (12)$$

where the Reynolds number for gas evolution is

$$Re_G = \frac{j_2 RTd}{(n/\nu)_B p \nu_L} \quad (13)$$

The mass transfer coefficient $k_b$ can be written explicitly

$$k_b = C_1 j_2^{0.5} \quad (14)$$

with

$$C_1 \equiv 1.89\left[\frac{RTD_C}{(n/\nu)_B F p d} f_G \theta^{0.5}(1-\theta^{0.5})\right]^{0.5} Sc_C^{-0.013} \quad (15)$$

### 3.4. *Combined mass transfer*

The overall mass transfer coefficient taking account of all separate mechanisms can be calculated from

$$k = (k_n^2 + k_v^2 + k_b^2)^{0.5} \quad (16)$$

Equation 16 was derived for a combination of two mass transfer coefficients [12] and has been confirmed experimentally [13] and theoretically [14].

## 4. Current efficiency equations

The current efficiency of copper deposition as defined by Equation 2 contains the partial current density of

deposition, $j_1$, given by Equation 3, where the mass transfer coefficient $k$ can be calculated from Equation 16. Inserting Equations 3 and 16 into Equation 2 gives

$$\epsilon = \frac{(n/\nu)_C F (k_n^2 + k_v^2)^{0.5} c_{C\infty} K_M}{j} \left[1 + \frac{k_b^2}{k_n^2 + k_v^2}\right]^{0.5} \tag{17}$$

Substituting the bubble-induced mass transfer coefficient, $k_b$, by means of Equation 14 and inserting Equation 2 in the form

$$\epsilon = 1 - \frac{j_2}{j} \tag{2a}$$

gives an inexplicit expression for the current efficiency dependent on the total current density

$$\epsilon = \frac{(n/\nu)_C F (k_n^2 + k_v^2)^{0.5} c_{C\infty} K_M}{j} \times \left[1 + (1 - \epsilon)\frac{C_1^2 j}{k_n^2 + k_v^2}\right]^{0.5} \tag{18}$$

With the abbreviations

$$K_1 \equiv \frac{(n/\nu)_C F (k_n^2 + k_v^2)^{0.5} c_{C\infty}}{j} K_M \tag{19}$$

and

$$K_2 \equiv \frac{C_1^2 j}{k_n^2 + k_v^2} \tag{20}$$

Equation 18 can be written

$$\epsilon = K_1 [1 + (1 - \epsilon) K_2]^{0.5} \tag{21}$$

With a parameter

$$X \equiv \frac{2}{K_1^2 K_2} \tag{22}$$

Equation 21 may be rewritten explicitly in terms of current efficiency

$$\epsilon = \left[K_1^2 + \frac{2}{X} + \frac{1}{X^2}\right]^{0.5} - \frac{1}{X} = \frac{[1 + 2X + (K_1 X)^2]^{0.5} - 1}{X} \tag{23}$$

Equation 23 is shown in Fig. 2. As seen from Equations 19, $K_1$ takes account of free and forced macroconvective mass transfer. Disregarding these two mass transfer mechanisms, i.e., setting $K_1 = 0$, results in

$$\epsilon = \frac{(1 + 2X)^{0.5} - 1}{X} \tag{24}$$

Equation 24 coincides with a current efficiency equation derived earlier [1]. In that paper the importance of the current efficiency for hydrogen evolution in mass transfer experiments was studied, and at that time it was common to attribute the action of mass transfer solely to bubble-induced microconvection. Equation 23 is an extension of the old solution by taking into account free and forced convective mass transfer in addition to bubble-induced effects.

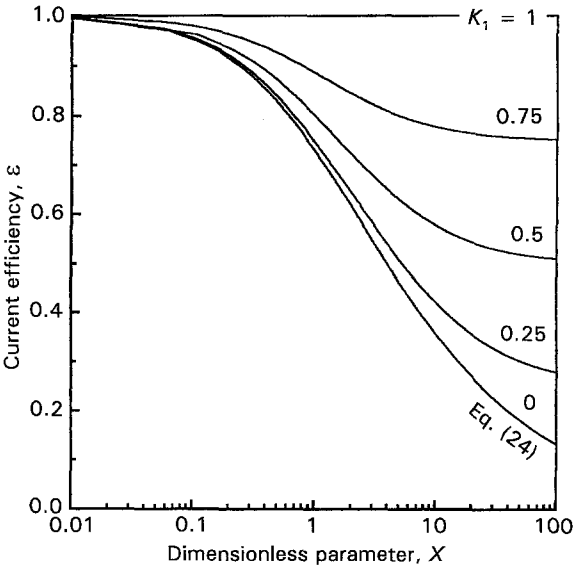


Fig. 2. Current efficiency as a function of the parameters $K_1$ and $X$, Equation 23.

Equations 23 and 24 relate the current efficiency to the total current density $j$. For practical use, the equations are problematic, because the parameter $C_1$ contained in the dimensionless parameter $K_2$ depends on the partial current density of hydrogen formation, $j_2$, for several reasons. The gas evolution efficiency, $f_G$, the bubble break-off diameter, $d$, and the fractional shielding, $\theta$, are all functions of $j_2$. It is advantageous to write Equation 23 in a different form as a function of the partial current density, $j_2$, of gas formation. Starting from Equation 17 and substituting $k_b$ by means of Equation 14 and $j$ by Equation 2(a) yields

$$\epsilon = \frac{1}{1 + K_3} \tag{25}$$

with a single dimensionless parameter

$$K_3 \equiv \frac{j_2}{(n/\nu)_C F (k_n^2 + k_v^2 + C_1^2 j_2)^{0.5} c_{C\infty} K_M} \tag{26}$$

The macroconvection mass transfer coefficient, $k_v$, is completely independent of both partial current densities, $j_1$ and $j_2$. As seen from Equation 4, the mass transfer coefficient of natural convection, $k_n$, only depends on $j_2$. (Moreover, its effect is small provided that $k_n \ll k_v$, as is the case in the present problem.) So Equation 26 is virtually independent of the partial current density for copper deposition, $j_1$, Equations 23 and 25 are identical and differ only in form. The advantage of Equation 25, shown in Fig. 3, is its easy applicability.

## 5. Comparison with experimental data

The restricted current efficiency Equation (Equation 24) which differs from the total equation (Equation 23) by

*Table 1. Data of Janssen's experiments [16] used for verification of Equation 23*

| | | |
|---|---|---|
| Bulk concentration $CuSO_4$ | $c_{Co} = 1000\,mol\,m^{-3}$ | [16] |
| Bulk concentration $H_2SO_4$ | $c_{\infty} = 1000\,mol\,m^{-3}$ | [16] |
| Temperature | $T = 50\,°C$ | [16] |
| Kinematic viscosity | $\nu_T = 0.73 \times 10^{-6}\,m^{-2}\,s^{-1}$ | [16] |
| Density | $\rho = 1190\,kg\,m^{-3}$ | [16] |
| Diffusion coefficient $Cu^{2+}$ | $D_C = 0.88 \times 10^{-9}\,m^{-2}\,s^{-1}$ | [16] |
| Diffusion coefficient $H_2$ | $D_B = 4.9 \times 10^{-9}\,m^{-2}\,s^{-1}$ | |
| Migration factor | $K_M = 1.08$ | [16] |

the forced convection term $k_v$, is applicable to an electrolyte in the absence of forced and natural liquid flow. It has been compared with experimental data of Sedahmed *et al.* [15] and has been found suitable for practical use in the absence of forced flow [1]. The more general Equation 23 can be tested in comparison with experimental data of Janssen [16] obtained with liquid flow at various velocities. The properties data used for verification of Equation 23 are listed in Table 1 and were mostly taken directly from Janssen [16].

Calculation of $k_v$ causes some difficulties. Values of the forced flow mass transfer coefficient of a cylindrical electrode have been obtained by Janssen [16], but unfortunately for a dilute copper solution [17], whereas the experimental current efficiency values published in [16] were obtained in concentrated solution. Values of the forced flow mass transfer coefficient, $k_v$, in the absence of gas evolution were, therefore, calculated from available mass transfer equations. Because of the complex geometry applied by Janssen it appeared reasonable to make use of different mass transfer equations, particularly that of Ulsamer [18] for a cylinder in an infinite flow and that of Gnielinski [19] for a cylinder in a channel. The separately obtained results do not differ greatly from each other, but are much lower than those of Janssen. The forced convection mass transfer coefficient used for evaluation of Equation 23 are $k_v = 22 \times 10^{-6}\,m\,s^{-1}$ for one of the sets of Janssen's experimental data with a nominal velocity of $v = 0.33\,m\,s^{-1}$, and $k_v = 37 \times 10^{-6}\,m\,s^{-1}$ for a second set of $v = 0.84\,m\,s^{-1}$. The mass transfer coefficient for liquid-phase natural convection, $k_n$, was calculated from Equation 4. The values turned out to be small enough compared with those of forced flow, $k_v$, to be of virtually no effect in the current density range applied. The mass transfer related to bubble evolution was calculated from Equation 12 with Equations 7 and 8.

The calculated partial current densities of both competing reactions are shown in Fig. 4. Reaction kinetic data for the hydrogen formation reaction were taken from Nieber [20]. The partial current density for copper deposition was calculated for the two flow velocities and the conditions of Janssen's experiments [16] from Equation 3 with Equations 14 and 16 for given values of the partial current density $j_2$. The cathode potential shown in Fig. 4 is of no effect on the interrelation of the partial current densities.

The calculated current efficiencies for the same two flow velocities are shown in Fig. 5, lines (b) and (c). They are compared with the experimental data points of Janssen [16].

## 6. Discussion

The restricted current efficiency Equation 24 based on the assumption that the mass transfer is controlled solely by bubble-induced microconvection, represents the lower bound of the current efficiency. This is shown in Fig. 5 as line (a).

The experimental values of the current efficiency obtained by Janssen [16] for two flow velocities are larger than line (a) thus confirming the beneficial effect of superimposed forced convection. The

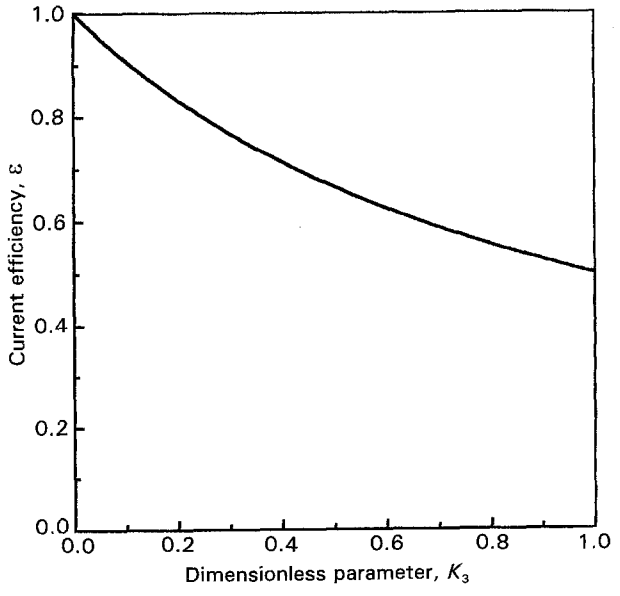


Fig. 3. Current efficiency as a function of the parameter $K_3$, Equation 25.

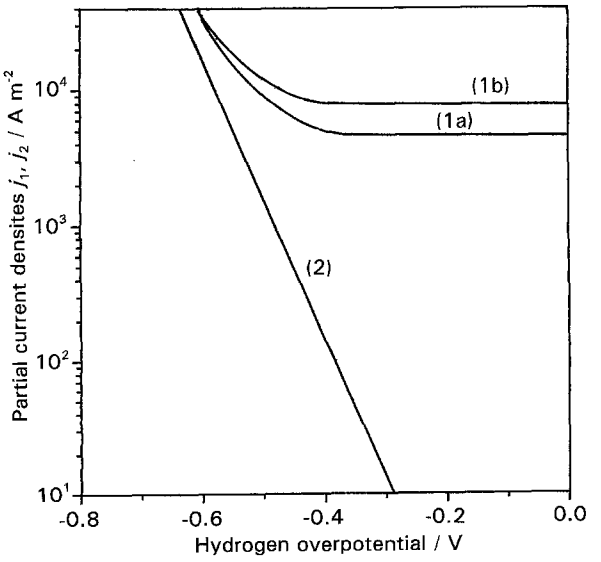


Fig. 4. Increase in partial current density of the copper deposition (1) as the gas evolution (2) attains large values. 1(a): calculated for the conditions of Janssen's experiments [16] for a nominal velocity $V = 0.33\,m\,s^{-1}$; 1(b): $v = 0.84\,m\,s^{-1}$.

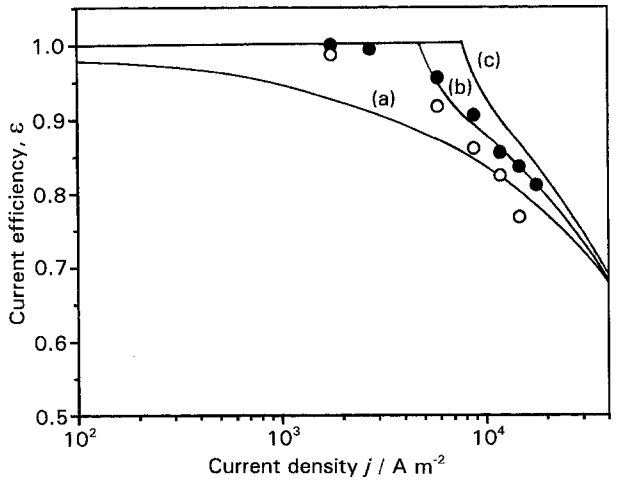


Fig. 5. The current efficiency as a function of the total current density, calculated from Equations 25 and 26. (a): $v = 0$; (b): $v = 0.33\,\mathrm{m\,s^{-1}}$. (c) $v = 0.84\,\mathrm{m\,s^{-1}}$. Experimental data points from Janssen [16], (○): $v = 0.33\,\mathrm{m\,s^{-1}}$; (●): $v = 0.84\,\mathrm{m\,s^{-1}}$.

experimental data are slightly lower than the theoretical lines (b) and (c) for both experimental sets of varying flow velocity. It is difficult to be certain whether the reason for this discrepancy is the unusual geometry used in the experiment or inaccuracy in the properties data used in the calculation, particularly in Equations 7 and 8.

Figure 5 expresses the well-known fact that the current efficiency generally decreases as the current density increases. But the effect is negligible at large values of flow velocity and moderate values of current density. As the current density increases, the mass transfer mechanism of bubble-induced microconvection becomes dominant. This is visible from the asymptotic approach of the forced flow lines (b) and (c) to line (a).

Equation 23 has been derived for the current efficiency of copper deposition. However, the equation is a general one and may be used for the prediction of current efficiency of other reactions accompanied by competing gas evolution.

## 7. Summary

The current efficiency Equation 23 or 25, derived theoretically, contains mass transfer coefficients associated with forced flow and natural flow in addition to that of bubble-induced microconvection. Thus, it takes account of all the three mass transfer mechanisms acting in copper deposition and is a generalization of the prior Equation 24 [1] considering microconvection alone.

Comparison with experimental results for electrodeposition of copper under forced flow conditions confirms the suitability of the improved current efficiency equation.

## References

[1] H. Vogt, *Surf. Technol.* **17** (1982) 301.
[2] C. Wagner, *Adv. Electrochem. Engng.* **2** (1962) 1.
[3] P. M. Robertson and O. Dossenbach, *Oberfläche-Surface* **22** (1981) 282.
[4] E. Baars and C. Kayser, *Z. Elektrochem.* **36** (1930) 428.
[5] H. Vogt, *Electrochim. Acta* **38** (1993) 1421.
[6] *Idem., Electrochim. Acta* **38** (1993) 1427.
[7] *Idem., Ber. Bunsenges. Phys. Chem.* **96** (1992) 158.
[8] *Idem., Electrochim. Acta* **29** (1984) 167.
[9] *Idem., J. Electrochem. Soc.* **137** (1990) 1179.
[10] H. Hausen, *Allg. Wärmetechnik* **9** (1959) 75.
[11] K. Stephan and H. Vogt, *Electrochim. Acta* **24** (1979) 11.
[12] H. Vogt, *ibid.* **23** (1978) 203.
[13] G. Bendrich, W. Seiler and H. Vogt, *Int. J. Heat Mass Transfer* **29** (1986) 1741.
[14] H. Vogt, *Electrochim. Acta* **32** (1987) 633.
[15] G. H. Sedahmed, Y. A. El-Taweel and O. A. Hassan, *Surf. Technol.* **14** (1981) 109.
[16] L. J. J. Janssen, *J. Appl. Electrochem.* **18** (1988) 339.
[17] *Idem.*, private communication (1988).
[18] J. Ulsamer, *Forsch. Ing.-Wes.* **3** (1932) 94.
[19] V. Gnielinski, *ibid.* **44** (1975) 145.
[20] F. Nieber, Diss. Techn. Hochschule Köthen (1993).